OENO One
vine & wine

DOI: https://doi.org/10.20870/oeno-one.2026.60.1.9377

OPEN ACCESS

ENOLOGY ORIGINAL RESEARCH ARTICLES

Photodegradation of riboflavin in white wine: impact of contrasting light sources and ethanol contents

Isara Vongluanngam[1,2,*], John W. Blackman[1], Leigh M. Schmidtke[1,2], Kerry L. Wilkinson[2,3], Xinyi Zhang[1], and Andrew C. Clark[1]

[1] Gulbali Institute, School of Agricultural, Environmental and Veterinary Sciences, Charles Sturt University, Locked Bag 588, Wagga Wagga, NSW 2678, Australia
[2] The Australian Research Council Training Centre for Innovative Wine Production, University of Adelaide (Waite Campus), SA 5064, Australia
[3] Discipline of Wine Science and Waite Research Institute, The University of Adelaide, PMB 1, Glen Osmond, SA 5064, Australia

Article number: 9377

*correspondence:
ivongluanngam@csu.edu.au

Associate editor:
Doris Rauhut

Received:
17 April 2025

Accepted:
23 December 2025

Published:
21 January 2026

This article is published under the **Creative Commons licence** (CC BY 4.0).

Use of all or part of the content of this article must mention the authors, the year of publication, the title, the name of the journal, the volume, the pages and the DOI in compliance with the information given above.

ABSTRACT

Riboflavin is a photoinitiator that is known to promote the accumulation of off-aroma compounds in white wine. However, the combined impact of different non-ionising radiation wavelengths and wine ethanol concentrations on this process is not well understood. An aqueous tartrate-buffer solution and a de-alcoholised Chardonnay (0.4 % *(v/v)*) wine, both supplemented with 0.5 mg/L riboflavin and adjusted to different ethanol concentrations (0.4 or 12.4 % *(v/v)*), were bottled with low oxygen concentrations. Samples were stored in darkness or exposed to different commercially available light sources (cool white fluorescent, cool white light-emitting diode (LED), and yellow LED). Concentrations of riboflavin were monitored over 7 and 14 days for the tartrate-buffer solutions and Chardonnay wines, respectively, while the Chardonnay wines also had measurements of volatile sulphur compounds and sensory analysis conducted at the end of the storage. Riboflavin degradation rates were highest when exposed to cool white LED, with progressively lower decay rates evident when exposed to cool white fluorescent or yellow LED, and for control samples stored in darkness. This order corresponded to increased photon energy within the wavelength range of 350–520 nm. After one day of exposure to cool white LED or fluorescent light, concentrations of hydrogen sulfide and methanethiol in the Chardonnay exceeded aroma threshold levels by 12-fold and 4-fold, respectively. The Chardonnay exposed to cool white LED was perceived to have 'sulphur/rotten egg' aroma, whereas exposure to cool white fluorescent light was associated with a 'cabbage' aroma. Ethanol only accelerated the loss of riboflavin in the Chardonnay exposed to cool white LED, but had little impact on volatile sulphur compound concentrations or the outcome of sensory evaluation. Exposure of the Chardonnay to yellow LED resulted in no reductive aromas being perceived by the sensory panel, which was consistent with the lower accumulation of volatile sulphur compounds and a decreased rate of riboflavin loss. As a consequence, a yellow LED source may offer considerable benefit when displaying wines in retail and consumer settings, where lighting is necessary.

KEYWORDS: light-struck aroma, photochemistry, wine storage, reductive aromas, no- and low-alcohol wine

INTRODUCTION

Riboflavin, also known as vitamin B2, is naturally present in fruits, vegetables, meat, dairy products, and fermented beverages (Combs, 2007; Ournac, 1968). In white wines, riboflavin concentrations typically range from 0.01 to 0.20 mg/L, depending on the yeast strain during alcoholic fermentation (Fracassetti *et al.*, 2017; Mattivi *et al.*, 2000) and may increase up to 0.25 mg/L or more during ageing on lees (Ournac, 1968). Riboflavin is highly photosensitive (Figure S1), and several factors can influence its light-induced degradation, including light intensity and wavelength, the matrix pH, viscosity, the availability of oxygen, oxidisable substrates and/or quenching compounds (Ahmad *et al.*, 2004; Choe *et al.*, 2005; Min & Boff, 2002; Sheraz *et al.*, 2014). Photochemical reactions are initiated when a reactant absorbs wavelengths of ultraviolet (UV) and/or visible light, and transitions to an excited electronic state (Figure S1) (Wardle, 2009). In a model wine solution, riboflavin favours the absorption of light at wavelengths around 370 and 442 nm, but can still absorb wavelengths up to 510 nm (Maujean & Seguin, 1983a). After absorbing light, riboflavin may reach an excited triplet state, whereby it becomes a potent oxidant able to react with various wine components. If it reacts with sulphur-containing amino acids, such as methionine, it can be detrimental to wine quality due to the formation of undesirable aroma compounds such as methional and its degradation product methanethiol (MeSH) (Figure S1) (Maujean & Seguin, 1983a). MeSH is thought to be the aroma compound most responsible for a fault commonly referred to as 'light-struck aroma' in wine, and MeSH imparts an aroma similar to that of cooked cabbage (Dozon & Noble, 1989). Hydrogen sulfide (H_2S) is another off-aroma compound generated in white wine exposed to light (Vongluanngam *et al.*, 2025); however, the mechanism of its formation is still unknown. Sparkling, and still white and rosé wines, particularly those produced with lees ageing, are known to be more susceptible to the occurrence of light-struck aroma (Haye *et al.*, 1977; Mattivi *et al.*, 2000; Mislata *et al.*, 2022).

Currently, the market for no and/or low (NOLO) alcohol beverages is experiencing dramatic growth (IWSR, 2023). NOLO production typically involves a post-fermentation processing stage to remove ethanol from wine. The commercial techniques commonly employed include membrane filtration (*e.g.*, reverse osmosis) or vacuum distillation (*e.g.*, spinning cone column), and they preserve most of the original desirable sensory qualities in the wine after the de-alcoholisation process (Catarino & Mendes, 2011; Longo *et al.*, 2017; Mangindaan *et al.*, 2018; Schmidtke *et al.*, 2012). However, the impact of light on de-alcoholised white wines has not been reported. This includes the impact of contrasting ethanol concentrations on the rate of riboflavin photodegradation or on the incidence and intensity of light-struck aroma.

Many white wines are bottled in transparent glass (*i.e.*, termed flint) and can be subjected to various types of lighting, including fluorescent and LED sources. Such exposure may occur in bottle shops, supermarkets, restaurants, or even during the storage of wine in residential environments. Flint bottles allow the maximum amount of light, with wavelengths above 300 nm, to be transmitted to the wine (Clark *et al.*, 2011; Vongluanngam *et al.*, 2024). As already mentioned, this light can have a detrimental photochemical impact on the sensory characteristics of wine. Fluorescent lighting, which is commonly used as lighting for commercial and residential environments, involves passing an electric current through mercury vapour that is held within a glass tube. This generates UV light that excites a phosphor coating on the inside of the glass tube, resulting in the emission of visible light (Mironava *et al.*, 2012). The overall spectrum of light emitted by fluorescent tubes typically features a series of sharp emission lines favoured by the excited phosphor coating and mercury vapour, which covers the UV – visible wavelength range. Fluorescent tubes with different profiles of emitted spectra of light are given different commercial names depending on the correlated colour temperature, such as 'warm white' (2,700–3,000 K), 'cool white' (4,000–4,500 K) and 'daylight' (5,000–6,500 K) (Borbély *et al.*, 2001; Ozenen, 2023). As an example of the emission spikes, the 'cool white' fluorescent tube has an emission spectrum with maxima at 313, 365, 405, 436, 480, 546, 578 and 580 nm (Fenton *et al.*, 2012; Spikes, 1981).

LED lighting involves the passage of an electric current through specific semiconductors that undergo electroluminescence, thereby releasing light. A spectrum of light emitted by an LED source is primarily within the visible wavelength range, but it will depend on the specific semiconductor and screening materials used in fabrication (Pearsall, 2010). For example, the commonly used 'cool white' LED lighting is made with a blue-emitting semiconductor (*i.e.*, indium gallium nitride or InGaN), coated with a phosphor material that converts blue light to a cooler white tone (Held, 2009). These types of LED sources generally have emission spectra with a maximum within 450–470 nm (Schubert, 2018). While previous studies have largely focused on the impact of sunlight and/or fluorescent light on the compositional and sensory changes of wine (Arapitsas *et al.*, 2020; Cáceres-Mella *et al.*, 2014; Carlin *et al.*, 2022; Fracassetti *et al.*, 2019; Lan *et al.*, 2021), few studies have investigated cool white LED lighting (Mislata *et al.*, 2022).

Another type of LED has been developed for use in wine cellars. These are LED lightings made from either gallium phosphide (GaP) or aluminium gallium indium phosphide (AlGaInP) that are coated with phosphor (Schubert, 2018) to enable emission of an 'amber' coloured visible light. This type of LED emits a spectrum of light within a narrow wavelength range of 570–590 nm; however, they cost around 20 times more than standard cool white LED sources. In this study, a more affordable commercial alternative, 'amber' LED lighting, which employs a yellow filter on a cool white LED to eliminate wavelengths below 500 nm, was used for comparison with other commercial light sources.

This work aimed to provide insights into two key gaps in knowledge that currently exist for the impact of light on white wine. That is, the comparative effect of different commercially available light sources on white wine, and the impact of ethanol (*i.e.*, 12.4 % *(v/v) versus* 0.4 % *(v/v)*). To achieve this aim, riboflavin-containing Chardonnay and tartrate-buffer solutions, at variable ethanol concentrations, were stored under cool white fluorescent, cool white LED and yellow LED tubes. Riboflavin degradation rates were determined in all samples, while H_2S and MeSH concentrations and sensory differences were also investigated for the Chardonnay wines.

MATERIALS AND METHODS

1. Chemicals

Potassium hydrogen tartrate (≥ 99 %), L-(+)-tartaric acid (≥ 99.5 %), riboflavin (≥ 99 %), sodium sulphide (≥ 99.5 %), and sodium methanethiolate (≥ 90 %) were all purchased from Sigma-Aldrich (Castle Hill, NSW, Australia). Ethanol (99.5 %) was obtained from ChemSupply (Gillman, SA, Australia). Methanol (LC grade solvent), acetonitrile (LC grade solvent), and glacial acetic acid were sourced from Honeywell (North Ryde, NSW, Australia), Sigma-Aldrich (Castle Hill, NSW, Australia), and Ajax Finechem (Taren Point, NSW, Australia), respectively. Solutions and dilutions were prepared using 18.2 Milli-Q water.

2. Sample preparations

All samples were prepared in an anaerobic hood, using nitrogen gas (99.99 % purity, BOC Gas & Gear, Wagga Wagga, NSW, Australia) to ensure oxygen minimisation, and the initial dissolved oxygen concentrations in the tartrate-buffer and wine samples were 0.22 ± 0.09 and 0.32 ± 0.07 mg/L, respectively. Oxygen concentrations were measured with a PSt3 oxygen sensor within a PSt3-oxygen sensor dipping probe and Fibox 4 trace meter (Precision Sensing GmbH, Regensburg, Germany). The tartrate-buffer solutions consisted of potassium hydrogen tartrate (0.011 M) and tartaric acid (0.008 M) added to either Milli-Q water or to 12 % *(v/v)* aqueous ethanol. The pH of these solutions was 3.2 ± 0.1, measured by a S20 SevenEasy™ pH meter (Mettler Toledo, Port Melbourne, VIC, Australia). The commercial wine used was a de-alcoholised 2024 Chardonnay (0.4 % *(v/v)* ethanol) labelled as a product of South Australia. It was originally bottled in 750 mL glass bottles sealed with screw cap closures. The general specification of the wine is shown in Table S1, and it was used without modifications of its pH (3.2) or sulphur dioxide concentration (*i.e.*, free SO_2 of 27 ± 3 mg/L, Table S2). Eight treatments (described in the following section) were prepared for the wine, and also for the tartrate-buffer, with each treatment consisting of three replicate bottles. Due to limited irradiated incubator capacity, treatments were prepared in four batches of two. For each de-alcoholised Chardonnay batch (*i.e.*, two treatments), three 750 mL bottles were opened and homogenised inside the anaerobic hood. Either water (266.4 mL) or ethanol (266.4 mL) was mixed with de-alcoholised wine (1,953.6 mL) to provide final alcohol concentrations of 0.4 % *(v/v)* and 12.4 % *(v/v)*, respectively, as measured using an Alcolyzer Module (Anton Paar GmbH, Graz, Austria). Three portions of 370 mL were then transferred into three separate 375 mL flint glass bottles (Plasdene Glass-Pak, Milperra, NSW) to provide the replicate bottles for a given treatment. Tartrate-buffer solutions (370 mL) were also aliquoted into 375 mL flint glass bottles. A riboflavin concentration of 0.5 mg/L, freshly prepared from an aqueous riboflavin stock solution (203 ± 3 mg/L), was added directly to all samples. This relatively high concentration enabled sufficient analysis time points to be conducted for accurate determination of the rapid riboflavin decay kinetics. It also facilitated the production of significant concentrations of detrimental sulfhydryl aroma compounds within the timeframe of the storage experiment. Each bottle was then sealed using screwcap closures with tin liners (Orora, Hawthorn, VIC, Australia) under a nitrogen gas atmosphere. The final concentrations of riboflavin were 0.50 ± 0.02 mg/L for the tartrate-buffer solutions and 0.56 ± 0.01 mg/L for the Chardonnay wines.

3. Experimental design

All samples (*i.e.*, tartrate-buffer solution (T), tartrate-buffer solution with 12 % *(v/v)* ethanol (TE), de-alcoholised wine with 0.4 % *(v/v)* ethanol (DA) and de-alcoholised wine with 12.4 % *(v/v)* ethanol (DA+E) were exposed to different commercial light sources from Philips lighting (Shanghai, China), being: a cool white fluorescent light tube (18 W, 1,350 lm, 4,000 K); cool white LED (8 W, 1,050 lm, 4,000 K), and LED with a yellow filter (10 W, 1,050 lm, 2,200 K) hereafter referred to as 'yellow LED' in this study. The emission spectrum of each light tube was measured over the wavelength range of 350–1000 nm (Figure 1A), determined by FieldSpec 4 (Malvern Panalytical Ltd., Worcestershire, UK) coupled to a VNIR (type 512 element silicon) photodiode array detector (Malvern Panalytical Ltd., Worcestershire, UK), and run by ViewSpec Pro version 6.2 software (Malvern Panalytical Ltd., Worcestershire, UK). Samples were positioned to receive a light intensity of 25 µmol/m²/s from each light source, measured by a LI-COR Biosciences LI-185A photometer (Lincoln, NE, USA). This intensity was chosen to provide a standardised experimental condition and falls within the range of typical illuminance observed for retail shelves in supermarkets and department stores, which has been reported to be approximately 5–30 µmol/m²/s (Jolley-Rogers *et al.*, 2017). During light exposure, all samples were maintained at 20 ± 2 °C inside a temperature-controlled incubator over a period of hours to 7 days for tartrate-buffer solutions (*i.e.*, T and TE) and a period of 1 to 14 days for the Chardonnay (*i.e.*, DA and DA+E). Control samples were stored under the same conditions but covered with aluminium foil to ensure darkness.

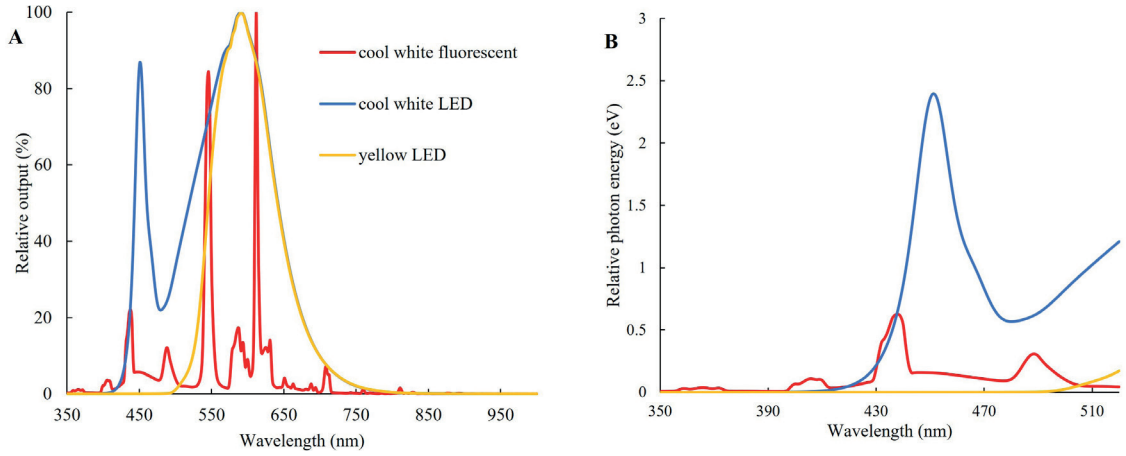


FIGURE 1. Emission spectra for the different light sources over a wavelength range of 350 to 1000 nm (A) and their relative photon energy spectra from 350 to 520 nm (B).

During sampling, nitrogen gas was continually blown into the top of the bottles for 5 min to minimise any increase in dissolved oxygen concentrations. Dissolved oxygen concentrations in all samples were maintained below 0.5 mg/L throughout the trial (data not shown). Another set of wine samples in each treatment was also prepared and exposed to either the cool white fluorescent or cool white LED sources for 1 day, or exposed to the yellow LED source or stored in darkness for 14 days without opening the bottles. These wine samples were then used for volatile sulphur compound analysis and sensory evaluation. Experimental factors were coded as shown in Table 1.

4. Chemical analysis

Ultrahigh-performance liquid chromatography (UPLC, Waters, Milford, USA), using a Waters Acquity BEH C18 column (2.1 mm, 50 mm, 1.7 µm, Waters, Milford, USA), connected to a photodiode array detector (PDA, Waters, Milford, USA), was used to measure concentrations of riboflavin as outlined in Dias *et al.* (2012). Free and total sulphur dioxide (SO_2) concentrations were measured using colorimetric test kits (Thermo Fischer Scientific, Scoresby, VIC, Australia) and a Konelab 20XT automated analyser (also Thermo Fisher Scientific). Total phenolic compounds (TPC) were determined by UV-visible spectrometry at a wavelength of 280 nm (Iland *et al.*, 2004). The volatile forms of H_2S and MeSH, subsequently referred to as 'free' forms within this study, were quantified by gas chromatography (GC, Agilent 7890B GC system, Agilent Technologies Australia, Mulgrave, VIC, Australia) coupled to a sulfur chemiluminescence detector (SCD, Agilent 355 SCD, Agilent Technologies Australia), using a DB-Sulfur SCD column (60 m, 0.32 mm, 4.2 µm, Agilent J&W Scientific, Agilent Technologies Australia). The analysis was conducted as per Kontoudakis *et al.* (2017), which is based on a modified protocol of Franco-Luesma and Ferreira (2014). Quantitation of the free sulfhydryl compounds was performed using ethyl methyl sulfide as an internal standard with internal standard curves prepared in either tartrate-buffer solution or tartrate-buffer solution with 12 % *(v/v)* ethanol for analysis of DA and DA+E samples, respectively.

5. Sensory analysis

Sensory analysis was performed after the exposure of wine samples to cool white fluorescent lighting for 1 day, cool white LED for 1 day, or yellow LED for 14 days. A control sample (*i.e.*, stored in darkness) also underwent sensory analysis at day 14. Pivot© Profile sensory methodology was utilised as outlined in Pearson *et al.* (2020). An experienced tasting panel was composed of 11 assessors (four females and seven males, aged 25–65), from Charles Sturt University and the Gulbali Institute (Wagga Wagga, NSW, Australia). All the panellists were familiar with the Pivot© Profile sensory method and had all previously been involved in sensory studies that had investigated reductive characters in wine. The sensory analysis was conducted in an open-plan, specialised sensory room at 20 ± 2 °C in two sessions; the four different DA samples (*i.e.*, F, L, Y and D) were assessed in the early afternoon, and the four different DA+E samples were evaluated in the late afternoon on the same day. A 30 mL volume of wine from a single bottle of each treatment was served in 220 mL ISO XL5 wine glasses labelled with random three-digit codes at ambient temperature, and extra wine was available upon request. Water and crackers were also provided. The panellists recorded differences in appearance, aroma, and palate descriptors when comparing the control pivot (*i.e.*, dark sample) to all the different treatments (*i.e.*, F, L, Y and D), according to Thuillier *et al.* (2015).

6. Statistical analysis

Statistical analyses were conducted using IBM SPSS Statistics software (version 27, Chicago, IL, USA). The paired-sample *t*-test was used to determine significant differences ($p < 0.05$) before and after light exposure in each treatment for total phenolic compounds, and free and total SO_2 concentrations. One-way analysis of variance (ANOVA) tests with post-hoc multiple comparisons were applied to assess the differences amongst rate constants and half-life data across treatments using Tukey's test for equal variances and Dunnett's T3, where unequal variances were evident. Correspondence analysis (CA) was performed on the sensory

TABLE 1. Experimental factors and sample codes.

Code	Lighting				Solution matrix		
	Cool white fluorescent (F)	Cool white LED (L)	Yellow LED (Y)	Dark (D)	Tartrate-buffer (T)	De-alcoholised Chardonnay (DA)	12 % *(v/v)* ethanol (E)
F/T	X				X		
F/TE	X				X		X
L/T		X			X		
L/TE		X			X		X
Y/T			X		X		
Y/TE			X		X		X
D/T				X	X		
D/TE				X	X		X
F/DA	X					X	
F/DA+E	X					X	X
L/DA		X				X	
L/DA+E		X				X	X
Y/DA			X			X	
Y/DA+E			X			X	X
D/DA				X		X	
D/DA+E				X		X	X

analysis data using Microsoft Office Excel version 2302 (Microsoft, Redmond, Washington, USA) installed with the XLSTAT statistical software (Lumivero, Denver, Colorado, USA). The quoted uncertainty is the standard deviation of three replications for a given treatment.

RESULTS AND DISCUSSION

1. Photodegradation of riboflavin

The emission characteristics of the cool white fluorescent, cool white LED, and yellow LED are shown in Figure 1A. The cool white fluorescent tube emitted wavelengths of light spanning the UV to visible range, with emission peaks at 409, 438, 488, 546, 588, 612 and 708 nm. In contrast, the cool white LED only emitted visible light within the 400–760 nm wavelength range, and had maxima at 451 and 591 nm, while the yellow LED only emitted light with wavelengths above 500 nm, and with a single maximum at 591 nm. As previously mentioned, the photochemical reaction is initiated by the absorption of light energy, typically in the form of photons, and the photon energy (E) can be calculated using $E = hc/\lambda$, where h is Planck's constant, c is the speed of light and λ is the wavelength. Figure 1B shows the relative photon energy spectra for each light source calculated over the wavelength range most relevant to the photoexcitation of riboflavin (*i.e.*, 350–520 nm). The integrated area under the spectra curves in Figure 1B corresponded to ratios for photon energies of 9:45:1 for cool white fluorescent:cool white LED:yellow LED.

The use of the tartrate-buffer solution allowed the composition of the sample matrix to be controlled for the preliminary experiments of this study, which focused on the impact of the different light sources and ethanol concentrations on riboflavin degradation. Figure 2A shows the rapid depletion of riboflavin in the tartrate-buffer solutions after only 2 h of exposure to the cool white LED or fluorescent light sources. This occurred regardless of the ethanol concentration of the samples. The yellow LED source led to slower riboflavin loss compared to the cool white fluorescent and cool white LED samples, but after seven days, 30–40 % more riboflavin was lost relative to samples stored in darkness (Figure 2B). As expected, the riboflavin concentrations in samples stored in darkness remained stable throughout the trial (*i.e.*, D/T and D/TE, Figure 2B).

Exposure of Chardonnay samples to the cool white LED or fluorescent light sources also resulted in riboflavin loss, with more than half the initial riboflavin being degraded within 5 h of irradiation, irrespective of the presence of ethanol. After this, the rate of riboflavin loss decreased (Figure 2C). Conversely, Chardonnay samples exposed to the yellow LED source (*i.e.*, Y/DA and Y/DA+E, Figure 2D) only had a 10 % loss in riboflavin concentration after 14 days of light exposure, again with no influence of ethanol concentration noted. No changes were observed in samples stored in darkness throughout the storage period (*i.e.*, D/DA and D/DA+E, Figure 2D).

The decrease in riboflavin concentration in the tartrate-buffer solution was best modelled by first-order kinetics (R^2 = 0.985–0.998, Table 2), in agreement with a previous

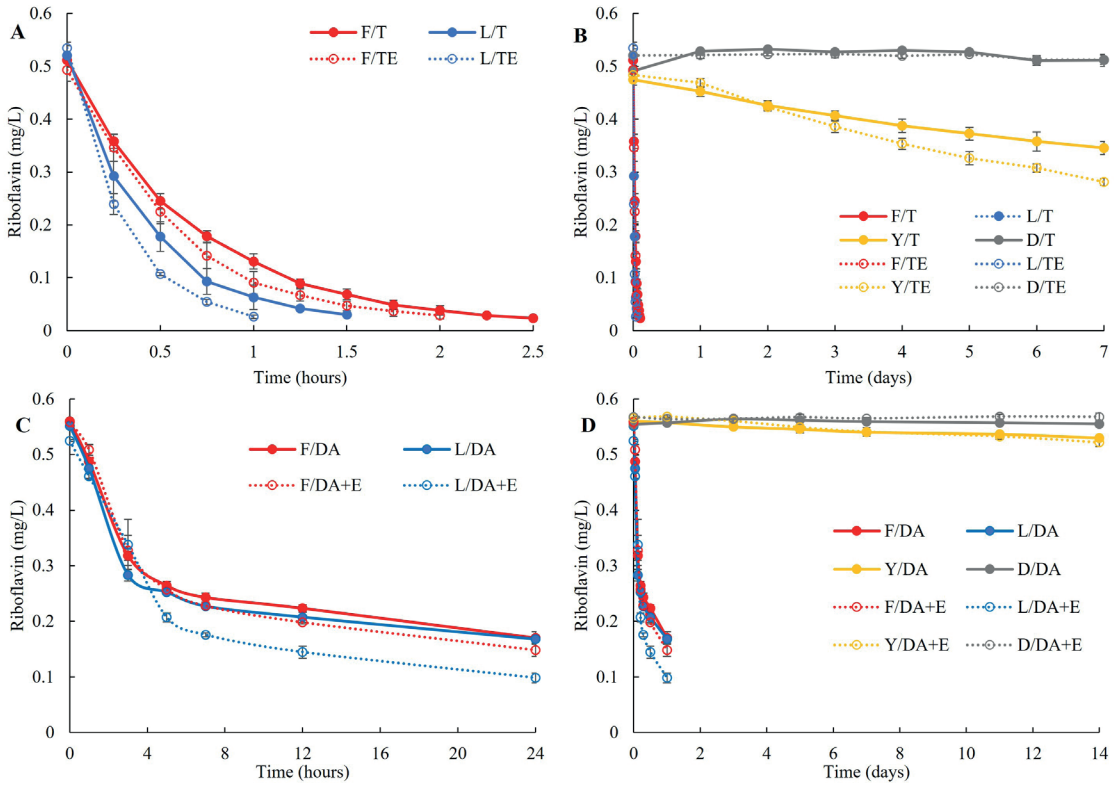


FIGURE 2. Concentrations (mg/L) of riboflavin in tartrate-buffer solutions (A, B) and Chardonnay wines (C, D) exposed to different light sources. A and C present compositional changes observed within 2.5 and 24 h, respectively, while B and D represent data collected throughout the storage period. Error bars represent the standard deviation (n = 3) from measurement of triplicate samples.

TABLE 2. The first-order decay rates and half-lives for riboflavin in tartrate-buffer solutions[a].

Treatment	Rate (days^{-1})	R^2	Half-life (days)
F/T	30 ± 3 c	0.995	0.023 ± 0.002 c
L/T	47 ± 6 b	0.985	0.015 ± 0.002 d
Y/T	0.046 ± 0.006 e	0.989	15 ± 2 a
F/TE	35 ± 3 c	0.988	0.020 ± 0.002 c
L/TE	72 ± 2 a	0.998	0.0096 ± 0.0003 e
Y/TE	0.081 ± 0.004 d	0.988	8.6 ± 0.5 b

[a] The rate constants and half-life data were treated with a log transformation to normalise the data prior to a one-way analysis of variance. Values followed by different letters indicate significant differences ($p < 0.05$) using Tukey's test for post-hoc multiple comparisons.

study (Fracassetti *et al.*, 2019). The tartrate-buffer solution exposed to cool white LED had the highest riboflavin decay rate, followed by fluorescent and yellow LED. This order for light sources was consistent with their corresponding photon energy emission over the wavelength range of 350–520 nm (Figure 1B). That is, the cool white LED source emitted a photon energy approximately 5-fold higher than for fluorescent and 45-fold higher than for the yellow LED. The presence of ethanol led to significantly ($p < 0.05$) faster degradation of riboflavin when the sample was exposed to light from cool white LED or yellow LED, but not light from cool white fluorescent tube. This difference is possibly due to the unique wavelengths less than 400 nm emitted by the cool white fluorescent tube compared to the other light sources. The half-life for riboflavin decay was approximately 1000-fold longer when the tartrate-buffer solution was exposed to the yellow LED compared to the cool white LED. The presence of ethanol decreased the riboflavin half-life by almost half, particularly when the sample was exposed to either the cool white LED (L/TE *vs* L/T, Table 2) or the yellow LED (Y/TE *vs* Y/T, Table 2). A previous study in a non-wine matrix reported that the decay rate of riboflavin in water was higher than in ethanol, and this was attributed to the lower viscosity of water (Ahmad *et al.*, 2015). However, the ethanol concentrations (*i.e.*, 100 *vs* 12 % *(v/v)*) and the pH (*i.e.*, 7 *vs* 3.2) reported by Ahmad *et al.* (2015) were different to those employed in the current study. A previous investigation also showed that the photodegradation of riboflavin in aqueous solutions became marginally slower as the pH increased from 3 to 4, but then rapidly increased from pH 6 to 10 (Ahmad *et al.*, 2004).

It was not possible to calculate the riboflavin decay rates for the Chardonnay samples exposed to yellow LED or stored in darkness, as ≤ 10 % of the riboflavin was degraded. For the remaining treatments, the riboflavin decay rate in Chardonnay appeared to have two distinct kinetic phases: the 0–7 h period, which has been assigned as the 1st phase, and the 7–24 h period assigned as the 2nd phase. The fit of modelled decay to the experimental data for these samples was better using second order (*i.e.*, $R^2 > 0.9$, Table 3) rather than first order or zero order (*i.e.*, $R^2 < 0.9$, data not shown) kinetics for both phases. This two-stage second-order kinetic behaviour of the riboflavin decay was in contrast to the decay in the tartrate-buffer solutions that showed single-stage first-order decay (Table 2). In a previous study reporting the photodegradation of riboflavin in Chardonnay wine (13 % *(v/v)* alcohol), riboflavin was also shown to follow second-order decay, albeit with only one kinetic phase rather than two (Vongluanngam *et al.*, 2024). For the Chardonnay treatments, the samples with higher alcohol and exposure to the cool white LED tube (L/DA+E) had the highest decay rates for both phases, consistent with the order of decay rates observed in the tartrate-buffer solutions treatments (*i.e.*, L/TE in Table 2). The half-lives calculated from the 1st phase of degradation were 3–5 h for the Chardonnay samples exposed to either cool white LED or fluorescent tube (Table 3). However, when the concentration of riboflavin fell below 0.25 mg/L, coinciding with the transition to the 2nd kinetic phase, the riboflavin half-life for these treatments extended from hours to a day or greater (Table 3).

The photo-induced loss of riboflavin in the Chardonnay was much slower than that observed in the tartrate-buffer solutions for a given light treatment. This was most likely due to the presence of phenolic compounds in the Chardonnay wine, as such compounds have been shown to effectively shield riboflavin from light exposure (Fracassetti *et al.*, 2019; Maujean & Seguin, 1983b). A significant decrease in total phenolic compounds ($p < 0.05$) was evident in the Chardonnay samples that had substantial riboflavin loss (*i.e.*, irradiated with the cool white light sources) (Table S2), with the largest decrease being for the L/DA+E treatment. The fate of these phenolic compounds was not determined, but it may have been a consequence of light-induced polymerisation or degradation reactions (Lan *et al.*, 2021), causing a decrease in their molar absorptivity at 280 nm. A decrease in total SO_2 concentration was also observed for the cool white light treatments (Table S2); however, there was no significant ($p < 0.05$) change in free SO_2 concentration. The different outcomes for free and total SO_2 may have been a consequence of weakly bound bisulphite adducts (*e.g.*, aldehydes and ketones) replenishing some of the free SO_2 lost due to light-induced effects (Waterhouse *et al.*, 2016).

2. Concentration of volatile sulphur compounds in Chardonnay samples

Free MeSH and H_2S are known to be key reductive off-aroma compounds generated during the photodegradation of riboflavin in white wine (Vongluanngam *et al.*, 2025). Quantification of these compounds was conducted at two time-points: at bottling and after the irradiation period; *i.e.*, day 1 for samples stored under the cool white LED or fluorescent light sources and day 14 for the samples stored under the yellow LED source or in darkness. At bottling, the concentrations of both H_2S and MeSH in DA and DA+E (Figures 3A and 3B) were considered low relative to their quoted aroma thresholds, *i.e.*, 1.6 and 3.1 µg/L, respectively (Siebert *et al.*, 2009; Solomon *et al.*, 2010).

After one day of cool white LED or fluorescent light exposure, the free MeSH concentration increased 3–4-fold above its aroma threshold in all wine samples, regardless of ethanol concentration (Figure 3A). No significant differences were observed in the free MeSH concentrations across the cool white lighting treatments, despite the differences in their riboflavin decay (Table 3). For the wine exposed to the yellow LED source for 14 days, the free MeSH concentration increased to twice the aroma threshold level; however, this only occurred in the higher ethanol concentration treatments (samples Y/DA+E in Figure 3A). The reason for this difference is not certain, especially given the similar decay rates of riboflavin under yellow LED (Y/DA and Y/DA+E

TABLE 3. The second-order decay rates and half-lives for riboflavin in the Chardonnay samples.

Treatment	Overall		1st phase			2nd phase		
	Rate[a] ($mg^{-1}·L·days^{-1}$)	R^2	Rate[b] ($mg^{-1}·L·days^{-1}$)	R^2	Half-life[c] (days)	Rate[d] ($mg^{-1}·L·days^{-1}$)	R^2	Half-life[e] (days)
F/DA	3.8 ± 0.4 b	0.867	8.5 ± 0.5 b	0.960	0.21 ± 0.01 a	2.6 ± 0.5 b	0.976	1.6 ± 0.3 a
L/DA	3.8 ± 0.2 b	0.815	9.3 ± 0.1 b	0.938	0.195 ± 0.004 a	2.2 ± 0.4 b	0.971	2.0 ± 0.4 a
F/DA+E	4.8 ± 0.5 b	0.909	9.5 ± 0.1 b	0.976	0.188 ± 0.002 a	3.4 ± 0.8 b	0.998	1.3 ± 0.3 ab
L/DA+E	8.4 ± 0.9 a	0.952	13.8 ± 0.6 a	0.966	0.138 ± 0.006 b	6 ± 1 a	0.997	0.9 ± 0.1 b

[a] The rate constant was calculated from data collected throughout the storage period (*i.e.*, 0–24 h), and Dunnett's T3 test was applied for post-hoc multiple comparisons.

[b] The rate constant was calculated from time-point 0–7 h, and Tukey's test was applied for post-hoc multiple comparisons.

[c] Dunnett's T3 test was applied for post-hoc multiple comparisons.

[d] The rate constant was calculated from time-point 7–24 h, and Tukey's test was applied for post-hoc multiple comparisons.

[e] Tukey's test was applied for post-hoc multiple comparisons.

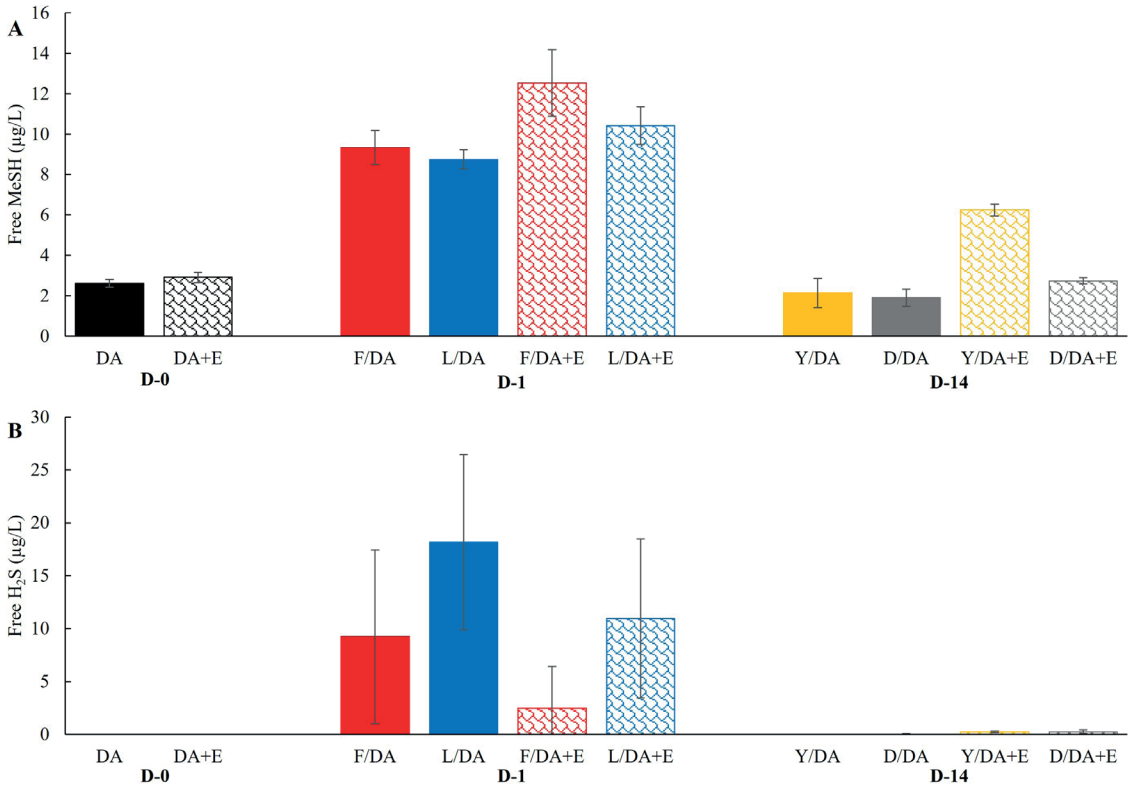


FIGURE 3. Concentrations (µg/L) of free MeSH (A) and free H_2S (B) in samples exposed to different light sources. Error bars represent the standard deviation (n = 3) for the measurement of triplicate samples within each treatment. F: fluorescent; L: LED; Y: yellow LED; D: dark; DA: de-alcoholised wine; DA+E: de-alcoholised wine added ethanol.

samples in Figure 1D), but it may be a consequence of ethanol impacting the yield of MeSH from methional (Figure S1). Trends for more MeSH with higher ethanol were also observed under fluorescent and cool white LED, though the differences were not significant, perhaps due to the shorter incubation period (1 day *vs* 14 days). The wine samples stored in darkness (D/DA and D/DA+E) showed no increase in MeSH concentration in the same period (Figure 3A).

Exposure of wines to the cool white light sources increased the free H_2S concentration far above the aroma threshold after one day, irrespective of ethanol concentrations (samples L/DA, F/DA, L/DA+E, and F/DA+E in Figure 3B). Although there were no significant differences in H_2S concentrations between treatments, there were trends to higher H_2S concentrations with cool white LED exposure and/or lower ethanol concentrations. The large uncertainty associated with the measurement of H_2S concentrations from wine samples exposed to light has been previously reported (Vongluanngam *et al.*, 2025). Factors contributing to the uncertainty may be the sensitivity of H_2S to oxygen ingress and/or H_2S being an intermediate species in a suite of photo-mechanistic pathways rather than a stable terminal product. As expected, the concentrations of H_2S in samples exposed to yellow LED and control samples remained relatively low (below aroma threshold levels) throughout the 14 days of storage (Figure 3B).

3. Sensory evaluation

A sensory panel characterised the wine samples using 22 descriptors for the de-alcoholised Chardonnay (DA) and 20 descriptors for the de-alcoholised Chardonnay with ethanol added (DA+E). Correspondence analysis (CA) was employed to analyse sensory data and produce Figures 4A and 4B. For the DA samples (Figure 4A), 95.86 % of variance was explained by Factor 1 (89.28 %) and Factor 2 (6.58 %), and 97.43 % of variance for DA+E samples (Figure 4B) was described by Factor 1 (85.90 %) and Factor 2 (11.53 %). The distribution of wine samples and descriptors in both Figures 4A and 4B suggested that Factor 1 was predominantly driven by the exposure of samples to wavelengths < 500 nm and associated with the photodegradation of riboflavin. Samples exposed to yellow LED, and samples stored in darkness, clustered on the left-hand side of this axis, were more closely associated with descriptors such as 'tropical/pineapple' and 'stone fruit'. This was the case for both 0.4 % *(v/v)* (Figure 4A) and 12.4 % *(v/v)* (Figure 4B) ethanol concentrations. The close proximity of these two treatments in both CA figures was a result of similar descriptors being assigned to them by the sensory panellists. These results were consistent with the lower concentrations of free H_2S and MeSH in the samples not exposed to cool white light, and therefore, reductive characters were not perceived. Although the sample with 12.4 % *(v/v)* ethanol and exposure to the yellow

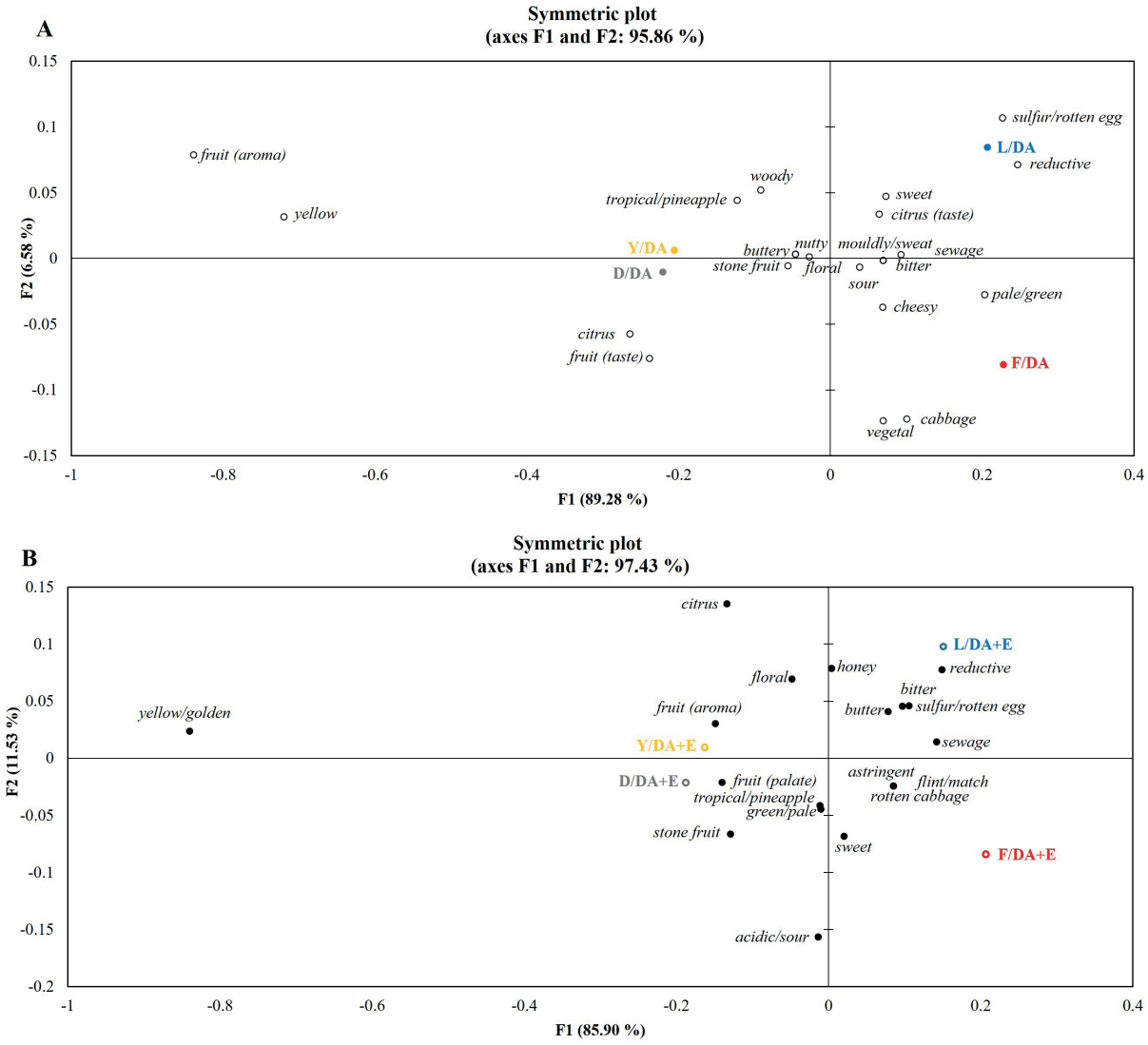


FIGURE 4. Correspondence analysis of de-alcoholised Chardonnay wine (DA) (A) and de-alcoholised Chardonnay with addition of ethanol (DA+E) (B) after 1 day of storage with exposure to either cool white LED (L) or fluorescent (F) light, or 14 days of storage with exposure to yellow LED (Y) or storage in darkness (D), using Pivot© Profile.

LED source accumulated a concentration of free MeSH that was marginally above the reported aroma threshold (sample Y/DA+E in Figure 3A), panellists did not report reductive characters in these samples.

Conversely, samples exposed to cool white LED and fluorescent light, irrespective of the presence of ethanol, were both located on the right-hand side of the Factor 1 axis and were associated with reductive attributes. Interestingly, Chardonnay samples irradiated by cool white LED were projected into the positive aspect of Factor 2 and associated with 'sulphur/rotten egg' and 'reductive' descriptors. This coincided with trends to higher H_2S production in the same samples (Figure 3B). Regardless of ethanol concentrations, Chardonnay samples exposed to fluorescent light were located lower on the Factor 2 axis and were more aligned with the 'cabbage' attribute. The association of cool white LED and fluorescent light-exposed samples with these reductive sensory features were consistent with the concentrations of MeSH and H_2S being well in excess of their corresponding aroma thresholds (Figures 3A and 3B). Panellists also rated the light-exposed wines, particularly those exposed to the cool white light treatments, as having less yellow colouration, which was consistent with previous studies (Cáceres-Mella *et al.*, 2014; Vongluanngam *et al.*, 2025).

CONCLUSION

The decay rates and half-lives of riboflavin in tartrate-buffer solutions and Chardonnay samples exposed to different commercial light sources have been established in this study. The photodegradation of riboflavin was more rapid when exposed to light sources that emitted higher photon energy within the 350–520 nm wavelength range. This meant that riboflavin decay rates were highest under cool white LED exposure, followed by cool white fluorescent, yellow LED, and darkness. The presence of ethanol only led significant acceleration of riboflavin photodegradation when the wine was exposed to a cool white LED source.

Free H_2S and MeSH concentrations increased above their aroma threshold levels after one day of cool white light exposure (LED or fluorescent), demonstrating the significant adverse impact that light exposure may have upon wine composition and sensory qualities. This was supported by sensory analysis, which attributed sulphur/rotten egg and/or cabbage-related descriptors to these samples.

The exposure of yellow LED resulted in considerably lower rates of riboflavin decay and may therefore offer considerable advantage for the display of wines within retail and consumer environments. However, the storage of wines in darkness still provided the best protection against the occurrence of light-struck aroma. While storage in complete darkness is optimal, yellow LED lighting may offer a practical alternative to standard cool white lighting in environments where lighting is necessary. While not suitable for general retail ambient lighting, yellow LED lighting could be particularly beneficial for wine cellar or refrigeration applications, offering a valuable tool in preserving wine quality. Future work should evaluate the long-term effects of these light sources on a variety of different white wines with varying riboflavin concentrations and light intensity conditions.

ACKNOWLEDGEMENTS

The research was conducted as part of the Australian Research Council Training Centre for Innovation Wine Production, funded by the Australian Government (www.ARCwinecentre.org.au; project number IC170100008).

REFERENCES

Ahmad, I., Anwar, Z., Ahmed, S., Sheraz, M. A., Bano, R., & Hafeez, A. (2015). Solvent effect on the photolysis of riboflavin. *AAPS PharmSciTech*, *16*(5), 1122-1128. https://doi.org/10.1208/s12249-015-0304-2

Ahmad, I., Fasihullah, Q., Noor, A., Ansari, I. A., & Ali, Q. N. M. (2004). Photolysis of riboflavin in aqueous solution: A kinetic study. *International Journal of Pharmaceutics*, *280*(1), 199-208. https://doi.org/10.1016/j.ijpharm.2004.05.020

Arapitsas, P., Dalledonne, S., Scholz, M., Catapano, A., Carlin, S., & Mattivi, F. (2020). White wine light-strike fault: A comparison between flint and green glass bottles under the typical supermarket conditions. *Food Packaging and Shelf Life*, *24*, 100492. https://doi.org/10.1016/j.fpsl.2020.100492

Borbély, Á., Sámson, Á., & Schanda, J. (2001). The concept of correlated colour temperature revisited. *Color Research and Application*, *26*(6), 450-457. https://doi.org/10.1002/col.1065

Cáceres-Mella, A., Flores-Valdivia, D., Laurie, V. F., López-Solís, R., & Peña-Neira, A. L. (2014). Chemical and sensory effects of storing Sauvignon Blanc wine in colored bottles under artificial light. *Journal of Agricultural and Food Chemistry*, *62*(29), 7255-7262. https://doi.org/10.1021/jf501467f

Carlin, S., Mattivi, F., Durantini, V., Dalledonne, S., & Arapitsas, P. (2022). Flint glass bottles cause white wine aroma identity degradation. *Proceedings of the National Academy of Sciences*, *119*(29). https://doi.org/10.1073/pnas.2121940119

Catarino, M., & Mendes, A. (2011). Dealcoholizing wine by membrane separation processes. *Innovative Food Science & Emerging Technologies*, *12*(3), 330-337. https://doi.org/10.1016/j.ifset.2011.03.006

Choe, E., Huang, R., & Min, D. B. (2005). Chemical reactions and stability of riboflavin in foods. *Journal of Food Science*, *70*(1), R28-R36. https://doi.org/10.1111/j.1365-2621.2005.tb09055.x

Clark, A. C., Dias, D. A., Smith, T. A., Ghiggino, K. P., & Scollary, G. R. (2011). Iron(III) tartrate as a potential precursor of light-induced oxidative degradation of white wine: Studies in a model wine system. *Journal of Agricultural and Food Chemistry*, *59*(8), 3575-3581. https://doi.org/10.1021/jf104897z

Combs, G. F., Jr. (2007). *The vitamins: Fundamental aspects in nutrition and health*. 3rd ed., Academic Press.

Dias, D. A., Smith, T. A., Ghiggino, K. P., & Scollary, G. R. (2012). The role of light, temperature and wine bottle colour on pigment enhancement in white wine. *Food Chemistry*, *135*(4), 2934-2941. https://doi.org/10.1016/j.foodchem.2012.07.068

Dozon, N. M., & Noble, A. C. (1989). Sensory study of the effect of fluorescent light on a sparkling wine and its base wine. *American Journal of Enology and Viticulture*, *40*(4), 265-271. https://doi.org/10.5344/ajev.1989.40.4.265

Fenton, L., Ferguson, J., & Moseley, H. (2012). Analysis of energy saving lamps for use by photosensitive individuals. *Photochemical & Photobiological Sciences*, *11*(8), 1346-1355. https://doi.org/10.1039/c2pp25035g

Fracassetti, D., Gabrielli, M., Encinas, J., Manara, M., Pellegrino, I., & Tirelli, A. (2017). Approaches to prevent the light-struck taste in white wine. *Australian Journal of Grape and Wine Research*, *23*(3), 329-333. https://doi.org/10.1111/ajgw.12295

Fracassetti, D., Limbo, S., Pellegrino, L., & Tirelli, A. (2019). Light-induced reactions of methionine and riboflavin in model wine: Effects of hydrolysable tannins and sulfur dioxide. *Food Chemistry*, *298*, 124952. https://doi.org/10.1016/j.foodchem.2019.124952

Franco-Luesma, E., & Ferreira, V. (2014). Quantitative analysis of free and bonded forms of volatile sulfur compounds in wine. Basic methodologies and evidences showing the existence of reversible cation-complexed forms. *Journal of Chromatography A*, *1359*, 8-15. https://doi.org/10.1016/j.chroma.2014.07.011

Haye, B., Maujean, A., Jacquemin, C., & Feuillat, M. (1977). Contribution à l'étude des « goûts de lumière » dans le vin de champagne *. 1. Aspects analytiques - Dosage des mercaptans et des thiols dans les vins. *OENO One*, *11*(3), 243-254. https://doi.org/10.20870/oeno-one.1977.11.3.1443

Held, G. (2009). *Introduction to light emitting diode technology and applications*. 1st edition, CRC Press. https://doi.org/10.1201/9781420076639

Iland, P., Bruer, N., Edwards, G., Weeks, S., & Wilkes, E. (2004). *Chemical analysis of grapes and wine: Techniques and concepts*. 2 ed., Patrick Iland Wine Promotions.

IWSR. (2023). *Key statistics: The no-alcohol and low-alcohol market*. Retrieved 31 May 2024 https://www.theiwsr.com/key-statistics-the-no-alcohol-and-low-alcohol-market/

Jolley-Rogers, C., Boland, L., & Bannister, P. (2017). Modelling for potential increases in lighting power density stringency in section J6 of the NCC. *AIRAH and IBPSA's Australasian Building Simulation 2017 Conference*, Melbourne, November 15-16, 1-16. https://www.airah.org.au/Common/Uploaded%20files/Archive/Conferences/2017/BS/TechnicalPapers/ABSC2017_TP_Jolley-Rogers.pdf?utm_source=rs.pdf

Kontoudakis, N., Guo, A., Scollary, G. R., & Clark, A. C. (2017). The impact of aging wine in high and low oxygen conditions on the fractionation of Cu and Fe in Chardonnay wine. *Food Chemistry*, *229*, 319-328. https://doi.org/10.1016/j.foodchem.2017.02.065

Lan, H., Li, S., Yang, J., Li, J., Yuan, C., & Guo, A. (2021). Effects of light exposure on chemical and sensory properties of storing Meili rosé wine in colored bottles. *Food Chemistry*, *345*. https://doi.org/10.1016/j.foodchem.2020.128854

Longo, R., Blackman, J. W., Torley, P. J., Rogiers, S. Y., & Schmidtke, L. M. (2017). Changes in volatile composition and sensory attributes of wines during alcohol content reduction. *Journal of the Science of Food and Agriculture*, *97*(1), 8-16. https://doi.org/10.1002/jsfa.7757

Mangindaan, D., Khoiruddin, K., & Wenten, I. G. (2018). Beverage dealcoholization processes: Past, present, and future. *Trends in Food Science & Technology*, *71*, 36-45. https://doi.org/10.1016/j.tifs.2017.10.018

Mattivi, F., Monetti, A., Vrhovšek, U., Tonon, D., & Andrés-Lacueva, C. (2000). High-performance liquid chromatographic determination of the riboflavin concentration in white wines for predicting their resistance to light. *Journal of Chromatography A*, *888*(1), 121-127. https://doi.org/10.1016/S0021-9673(00)00561-6

Maujean, A., & Seguin, N. (1983a). Contribution à l'étude des goûts de lumière dans les vins de Champagne. 3. Les réactions photochimiques responsables des goûts de lumière dans le vin de Champagne. *Sciences des Aliments*, *3*, 589-601.

Maujean, A., & Seguin, N. (1983b). Contribution à l'étude des goûts de lumière dans les vins de Champagne. 4. Approches a une solution œnologique des moyens de prévention des goûts de lumière. *Sciences des Aliments*, *3*, 603-613.

Min, D. B., & Boff, J. M. (2002). Chemistry and reaction of singlet oxygen in foods. *Comprehensive Reviews in Food Science and Food Safety*, *1*, 58-72. https://doi.org/10.1111/j.1541-4337.2002.tb00007.x

Mironava, T., Hadjiargyrou, M., Simon, M., & Rafailovich, M. H. (2012). The effects of UV emission from compact fluorescent light exposure on human dermal fibroblasts and keratinocytes *in vitro*. *Photochemistry and Photobiology*, *88*(6), 1497-1506. https://doi.org/10.1111/j.1751-1097.2012.01192.x

Mislata, A. M., Puxeu, M., Nadal, M., de Lamo, S., Mestres, M., & Ferrer-Gallego, R. (2022). Influence of different types of LEDs lights on the formation of volatile sulfur compounds in white and rosé wines. *Food Chemistry*, *371*, 131144-131144. https://doi.org/10.1016/j.foodchem.2021.131144

Ournac, A. (1968). Riboflavin pendant la fermentation du jus de raisin et la conservation du vin sur lies. *Annales de Technologie Agricole*, *17*, 67-75.

Ozenen, G. (2023). *Architectural Interior Lighting*. 1st ed. 2023, Springer Nature Switzerland. https://doi.org/10.1007/978-3-031-49695-0_1

Pearsall, T. (2010). *Photonics Essentials*. 2nd ed., McGraw-Hill, 320 p. ISBN 9780071629355.

Pearson, W., Schmidtke, L., Francis, I. L., & Blackman, J. W. (2020). An investigation of the Pivot© Profile sensory analysis method using wine experts: Comparison with descriptive analysis and results from two expert panels. *Food Quality and Preference*, *83*, 103858. https://doi.org/10.1016/j.foodqual.2019.103858

Schmidtke, L., Blackman, J., & Agboola, S. (2012). Production technologies for reduced alcoholic wines. *Journal of Food Science*, *77*(1), R25-R41. https://doi.org/10.1111/j.1750-3841.2011.02448.x

Schubert, E. F. (2018). *Light-Emitting Diodes*. 3rd ed., E. Fred Schubert, 672 p. ISBN 9780986382666.

Sheraz, M. A., Kazi, S. H., Ahmed, S., Anwar, Z., & Ahmad, I. (2014). Photo, thermal and chemical degradation of riboflavin. *Beilstein Journal of Organic Chemistry*, *10*(1), 1999-2012. https://doi.org/10.3762/bjoc.10.208

Siebert, T., Bramley, B., & Solomon, M. R. (2009). Hydrogen sulfide: Aroma detection threshold study in white and red wines. *AWRI Technical Review*, *183*, 14-16.

Solomon, M. R., Geue, J., Osidacz, P., & Siebert, T. E. (2010). Aroma detection threshold study of methanethiol in white and red wine. *AWRI Technical Review*, *186*, 8-10.

Spikes, J. D. (1981). Photodegradation of foods and beverages. In: *Photo-chemical and photobiological reviews*. Smith, K. C. ed., Vol. 6, Springer, New York. https://doi.org/10.1007/978-1-4684-7003-1_2

Thuillier, B., Valentin, D., Marchal, R., & Dacremont, C. (2015). Pivot© profile: A new descriptive method based on free description. *Food Quality and Preference*, *42*, 66-77. https://doi.org/10.1016/j.foodqual.2015.01.012

Vongluanngam, I., Blackman, J. W., Zhang, X., Schmidtke, L. M., Wilkinson, K. L., & Clark, A. C. (2025). Impact of Cu fractions on the light-induced spoilage aromas of Chardonnay wine at variable riboflavin concentrations. *Journal of Agricultural and Food Chemistry*, *73*(8), 4859-4868. https://doi.org/10.1021/acs.jafc.4c11032

Vongluanngam, I., Zhang, X., Blackman, J. W., Schmidtke, L. M., Wilkinson, K. L., & Clark, A. C. (2024). Impact of light on protective fractions of Cu in white wine: Influence of oxygen and bottle colour. *Food Chemistry*, *452*, 139504. https://doi.org/10.1016/j.foodchem.2024.139504

Wardle, B. (2009). *Principles and applications of photochemistry*. John Wiley & Sons, Ltd., 272 p. ISBN 9780470710135.

Waterhouse, A. L., Sacks, G. L., & Jeffery, D. W. (2016). *Understanding Wine Chemistry: Part B Chemistry of wine production processes*. John Wiley & Sons, Incorporated. https://doi.org/10.1002/9781118730720